Supporting Information

Study of GUPT-2, a Water-Stable Zinc-based Metal–Organic Framework as a Highly Selective and Sensitive Fluorescence Sensor in the Detection of Al^{3+} and Fe^{3+} Ions

San-Tai Wang[†,‡], Xiao Zheng[‡], Shu-Hua Zhang,[†,‡,*] Guangzhao Li[†], Yu Xiao[ϯ,*]

[†]*College of Chemistry, Guangdong University of Petrochemical Technology, Maoming, Guangdong, 525000, People's Republic of China*

[‡]*Guangxi Key Laboratory of Electrochemical and Magnetochemical Functional Materials(College of Chemistry and Bioengineering), Guilin University of Technology, Guilin 541004, People's Republic of China.*

[ϯ]*College of Environmental Science and Engineering, Guangdong University of Petrochemical Technology, Maoming, Guangdong, 525000, People's Republic of China*

Correspondence author e-mail: *E-mail:* zhangshuhua@gdupt.edu.cn (S. Zhang), Xiaoyu@gdupt.edu.cn (Y. Xiao).

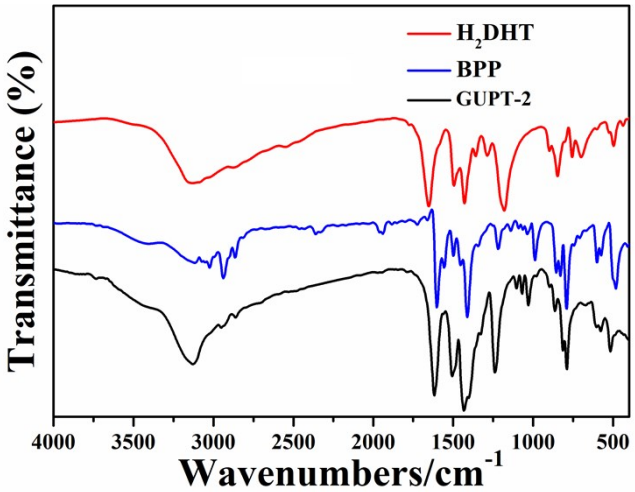

Fig. S1 IR spectra of **GUPT-2**, H_2DHT ligand and BPP ligand.

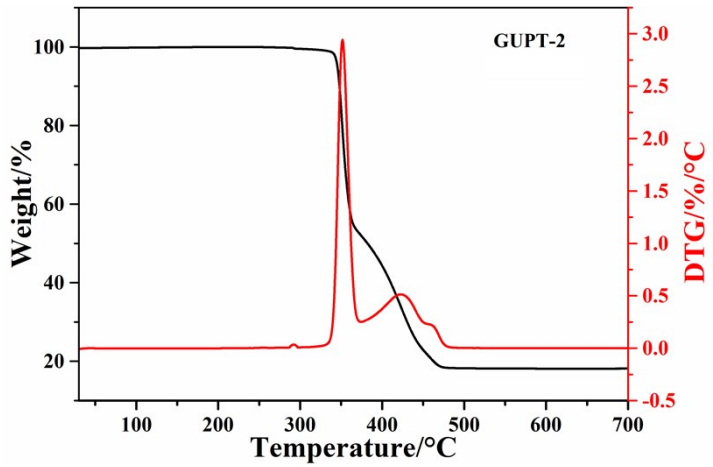

Fig. S2 The TGA and DTG plots of **GUPT-2**.

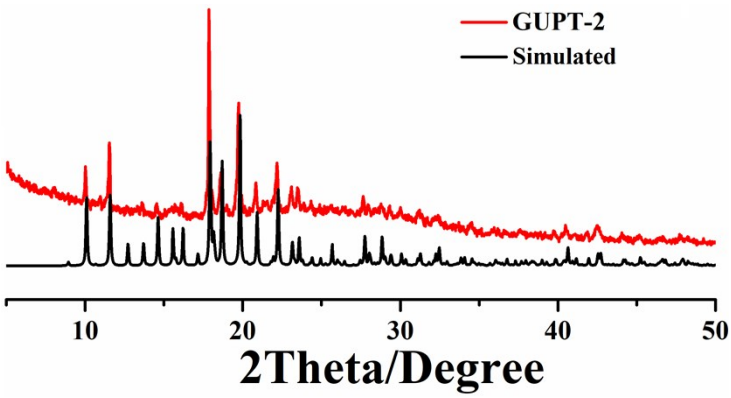

Fig. S3 Powder X-ray diffraction patterns for **GUPT-2**.

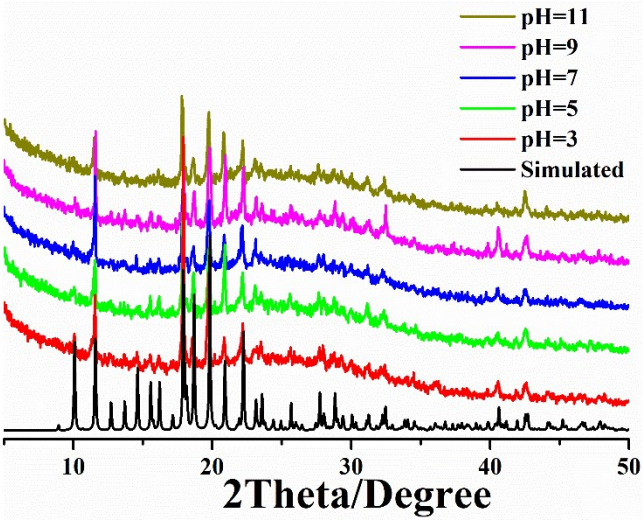

Fig. S4 Powder XRD patterns of **GUPT-2** immersed in different pH values.

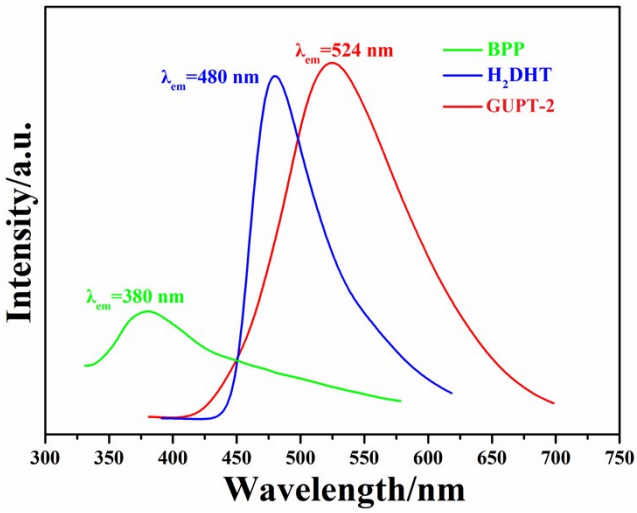

Fig. S5 Solid state emission spectra of **GUPT-2**, free H_2DHT ligand and BPP linker upon excitation at 360 nm, 370 nm and 310 nm, respectively.

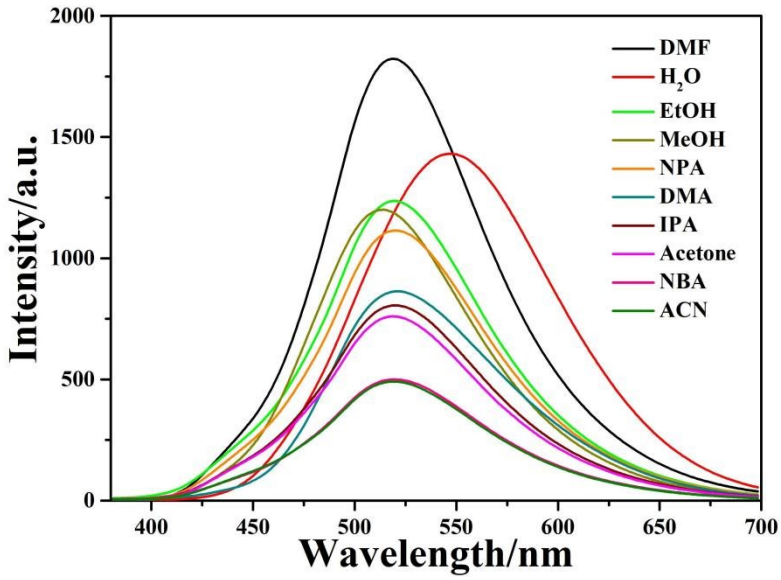

Fig S6 Emission spectra of **GUPT-2** dispersed in different solvents when excited at 360 nm.

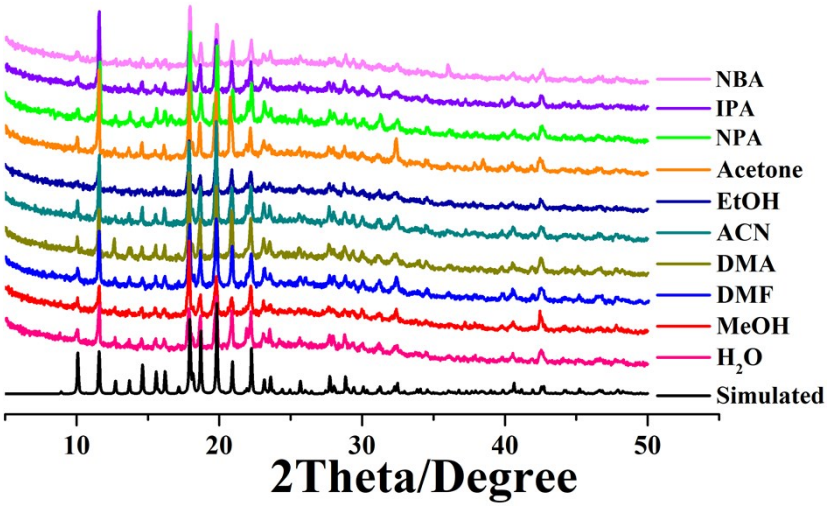

Fig. S7 Powder XRD patterns of **GUPT-2** immersed in different solvents at room temperature.

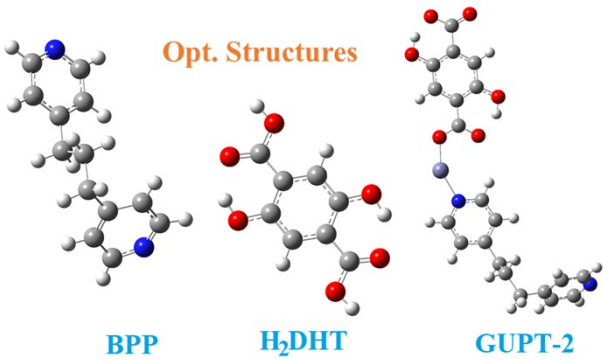

Fig. S8 Optimized structures of BPP linker, H_2DHT ligand and **GUPT-2**

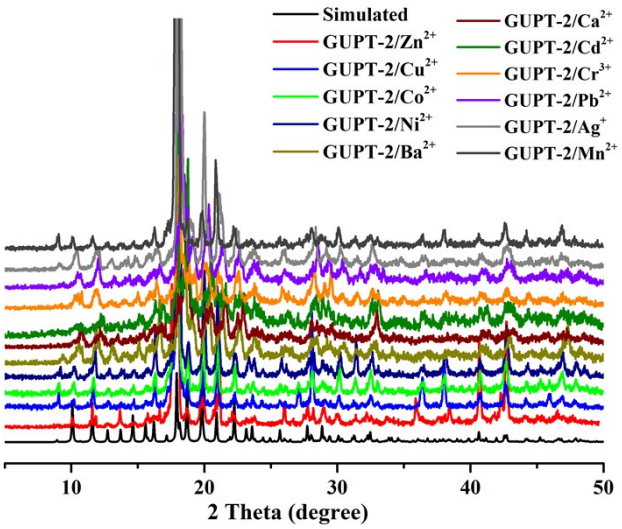

Fig. S9 Powder XRD patterns of **GUPT-2** immersed in different mental ions at room temperature.

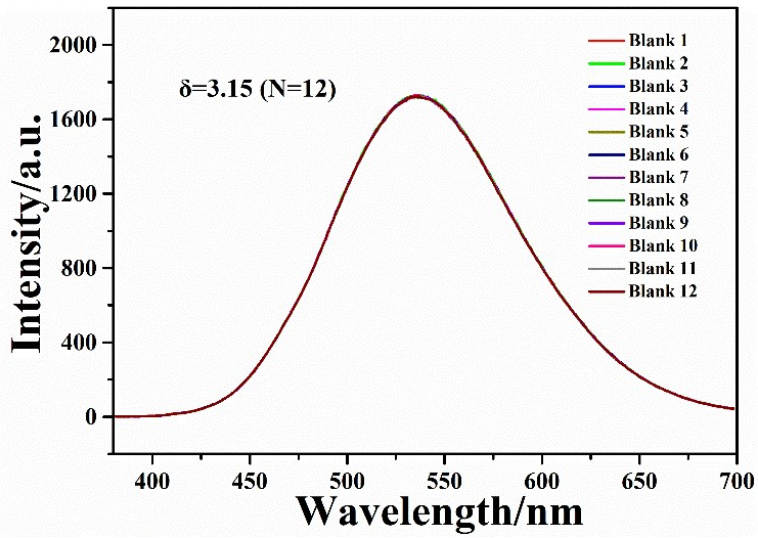

Fig. S10 The fluorescence spectra of blank **GUPT-2** (1 mg·mL^{-1}) at different measurements.

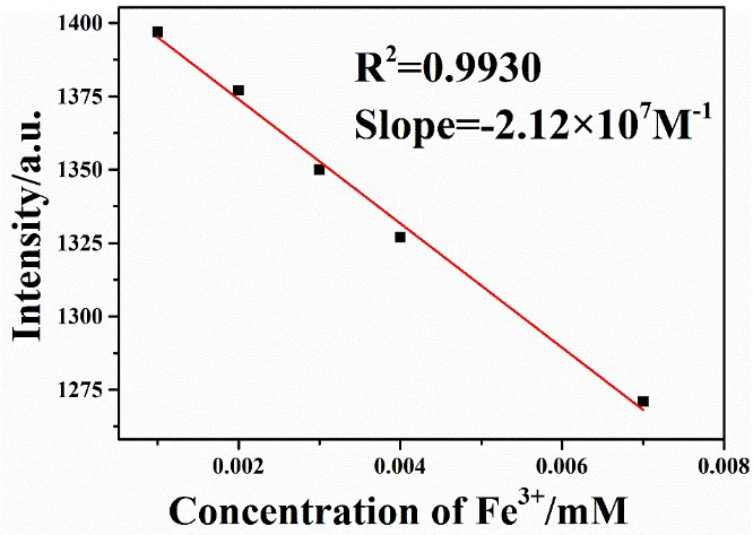

Linear Equation: Y = -21169X + 1416.38

R^2 = 0.9930

Slope = -2.12× 10^7 M^{-1}

δ=3.15 (N=12)

Limit detection =3δ/Slope=0.446 μM

Fig. S11 The fitting curve of the luminescence intensity of **GUPT-2** at different Fe^{3+} concentration

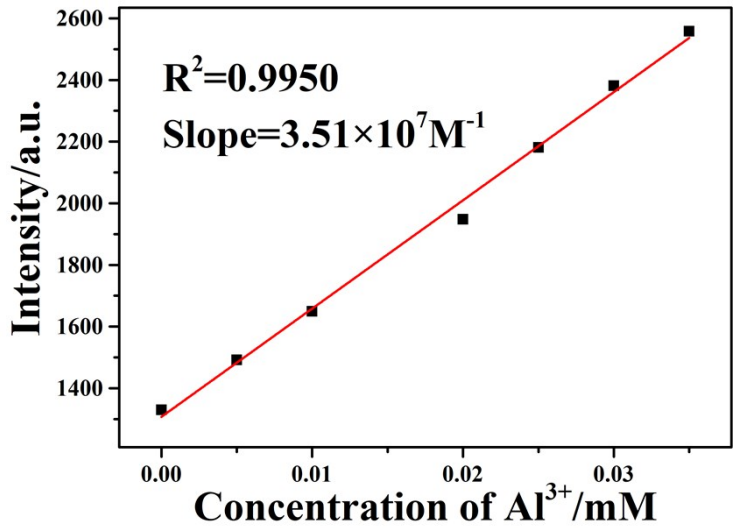

Linear Equation: Y = 35121X + 1306.96

R = 0.9950

Slope = 3.51× 10^7 M^{-1}

δ=3.15 (N=12)

Limit detection =3δ/Slope=0.269 μM

Fig. S12 The fitting curve of the luminescence intensity of **GUPT-2** at different Al^{3+} concentration

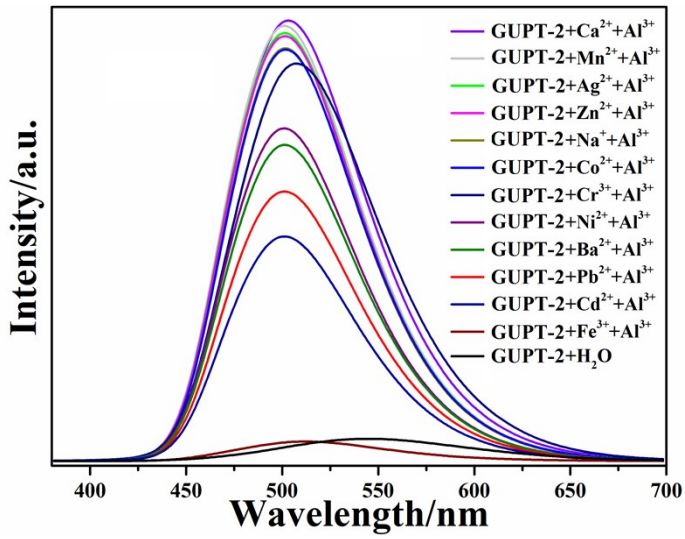

Fig. S13 The luminescence of intensity of interacting with different metal ions in water solution with and without Al^{3+} ions.

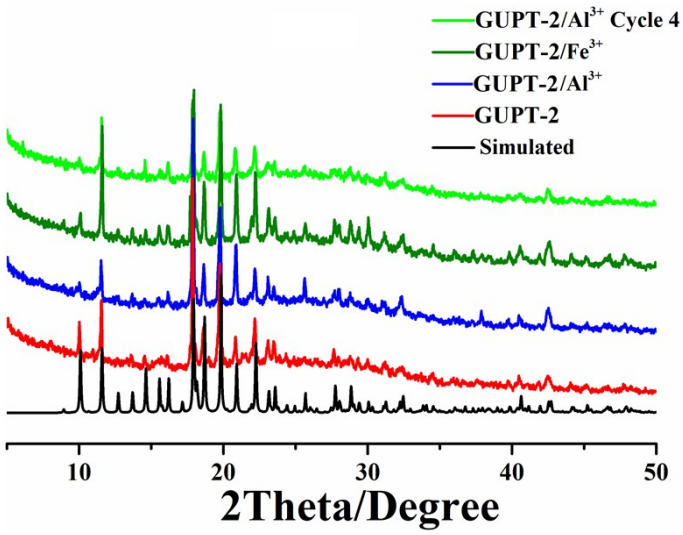

Fig. S14 Powder XRD patterns of simulated from the single-crystal data of **GUPT-2**, synthesized compound and **GUPT-2**/M^{n+}

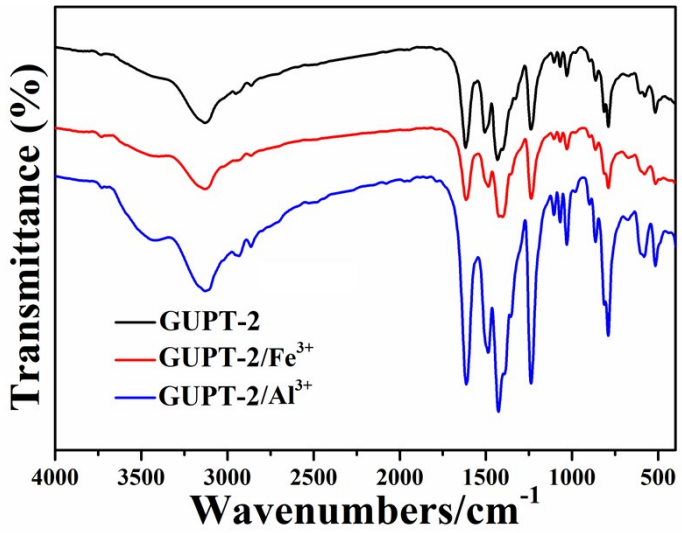

Fig. S15 IR spectra of Zn-MOF/Al^{3+} and Zn-MOF, respectively.

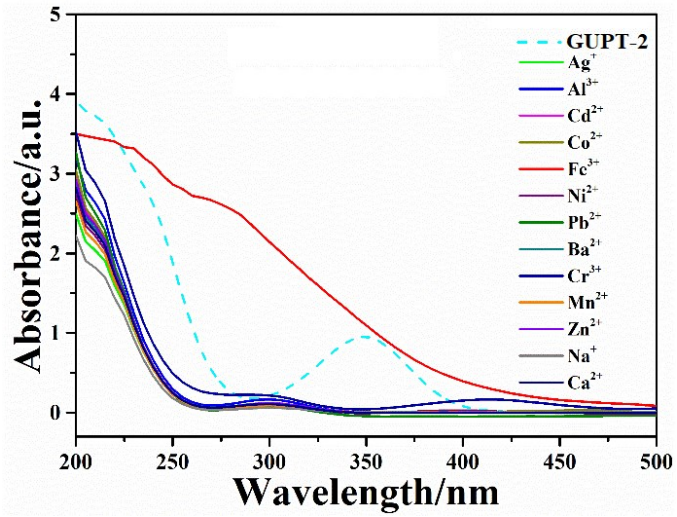

Fig. S16 UV-vis adsorption spectra of metal ions in water (10^{-3} mol/L) and the excitation spectrum of **GUPT-2** dispersed in aqueous solution.

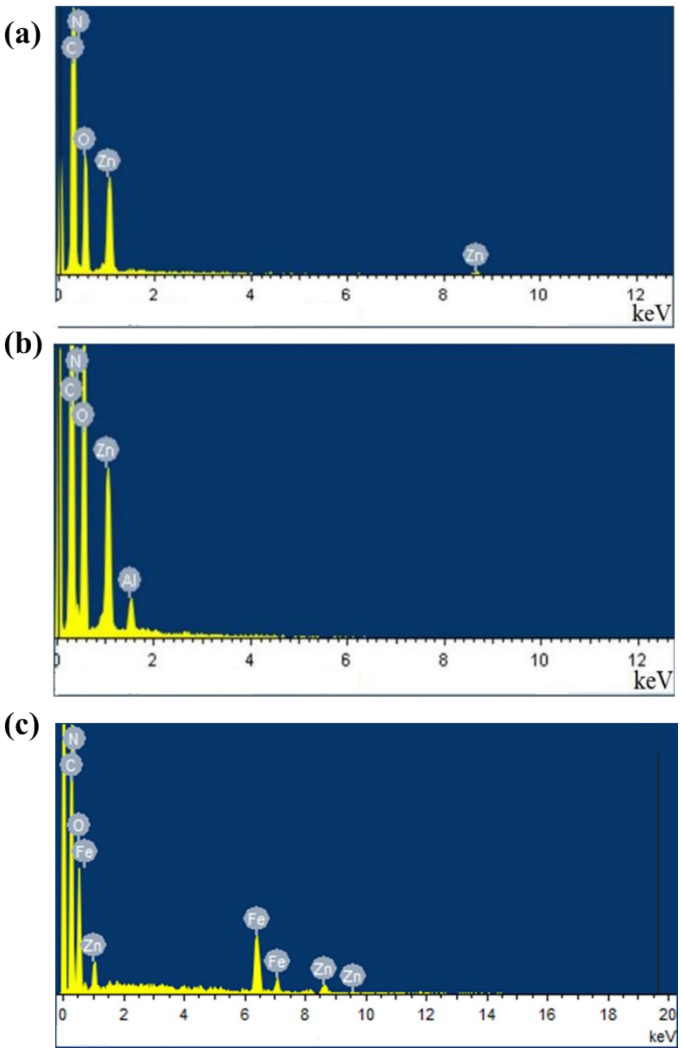

Fig. S17 EDS spectra of **GUPT-2** before (a) and after the sensing of Al^{3+}(b) and Fe^{3+}(c).

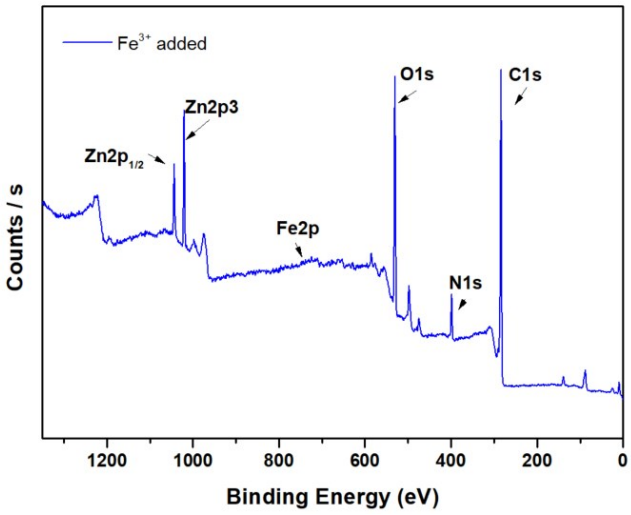

Fig. S18 XPS spectra of GUPT-2 after the sensing of Fe^{3+}.

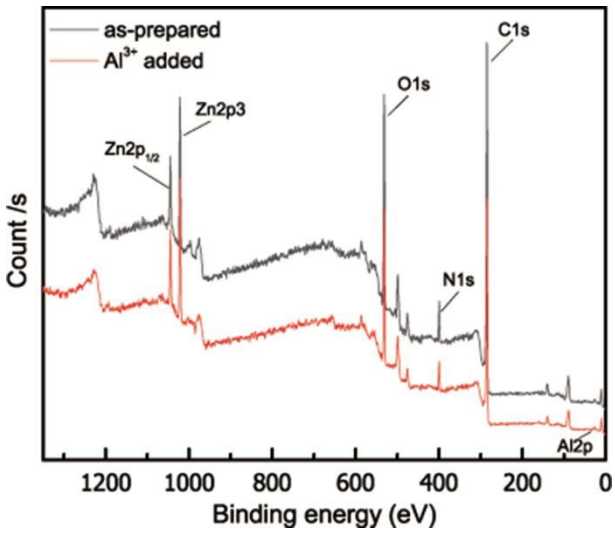

Fig. S19 XPS spectra of **GUPT-2** after the sensing of Al^{3+}.

Table S1 Selected bond lengths (Å) and angles (°) for **GUPT-2**.

Zn1−N1	2.056(4)	O2−Zn1−O5A	142.5(3)
Zn1−O2	1.950(3)	O2−Zn1−N2B	97.25(16)
Zn1−O5A	1.973(6)	O5A−Zn1−N1	91.4(2)
Zn1−N2B	2.041(4)	O5A−Zn1−N2B	109.1(2)
O2−Zn1−N1	106.19(16)	N2B−Zn1−N1	106.94(18)

Symmetry codes: (A) *x*, −*y*+1/2, *z*+1/2; (B) *x*−1, *y*, *z*.

Table S2 Hydrogen bond parameters for **GUPT-2**

D–H···A	d(D–H)	d(D···A)	d(H···A)	<(DHA)
O(3)–H(3)···O(1)	0.82	2.572(7)	1.84	147
O(4)–H(4)···O(6)	0.82	2.526(8)	1.79	148

Table S3 TD-DFT calculated main emission energies (nm) and electronic transitions of **GUPT-2**, H_2DHT and BPP ligands.

Compounds	Calcd. λ (nm)	Exp. λ (nm)	Significant contributions /Osc. Strengths (f)
GUPT-2	491	524	HOMO→LUMO+1 (99.8%)/0.1839
H_2DHT	487	480	HOMO→LUMO (99%) / 0.1561
BPP	350	380	HOMO→LUMO (98.7%)

Table S4 Highly Occupied and Lowest Unoccupied Molecular Orbitals for all ligands involved in the main luminescent charge transitions.

H_2DHT		**BPP**	
MO's	**Energy (eV)**	**MO's**	**Energy (eV)**

LUMO	-2.79	LUMO	-1.19
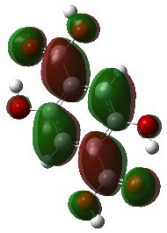		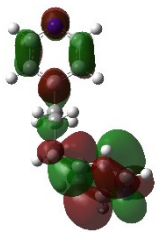	
HOMO	-6.31	HOMO	-7.16
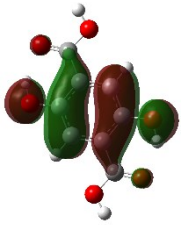		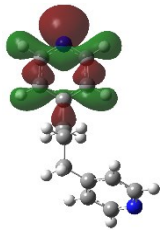	

Table S5 Vertical excitation energies (Eex), oscillator strengths (f), and Key transitions of the lowest few excited singlets obtained from TDDFT calculations of **GUPT-2**.

$E_{excitation}$ (eV)	excitation (nm)	Osc. Strength (f)	Key transitions	Orbital contribution
3.4305	361.42	0.1202	HOMO→LUMO	0.040
			HOMO→LUMO+1	0.941
5.0392	246.04	0.3006	HOMO-5→LUMO+1	0.77
			HOMO-2→LUMO+2	0.05
			HOMO→LUMO+5	0.12
5.3207	233.02	0.1331	HOMO-8→LUMO	0.46
			HOMO-5→LUMO+2	0.05
			HOMO→LUMO+6	0.32
			HOMO→LUMO+7	0.10
			HOMO→LUMO+8	0.02
5.8060	213.54	0.1844	HOMO-11→LUMO+1	0.05
			HOMO-5→LUMO+1	0.03
			HOMO→LUMO+6	0.05
			HOMO→LUMO+7	0.51
			HOMO→LUMO+8	0.31

Table S6 The energy values of some HOMO-LUMO of **GUPT-2**.

MO's	Energy (eV)
LUMO+5	-0.41
LUMO+4	-0.75
LUMO+3	-0.97
LUMO+2	-1.11
LUMO+1	-1.50
LUMO	-1.72
HOMO	-5.40
HOMO-1	-6.18

HOMO-2	-6.46
HOMO-3	-6.52
HOMO-4	-6.93
HOMO-5	-6.98

Table S7 Some HOMO and LUMO of **GUPT-2**.

HOMO	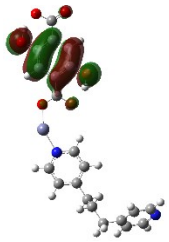	LUMO+5	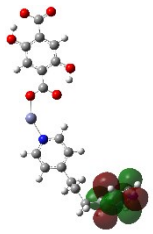
HOMO-1	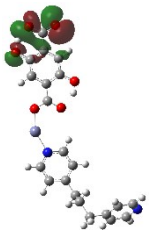	LUMO+4	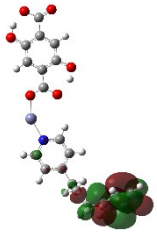
HOMO-2	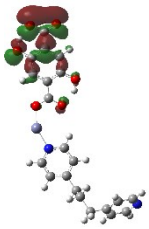	LUMO+3	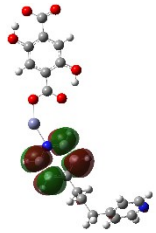
HOMO-3	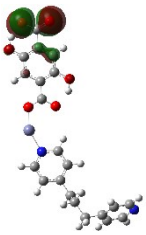	LUMO+2	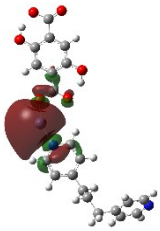
HOMO-4	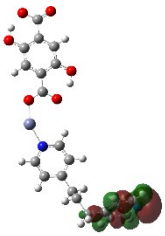	LUMO+1	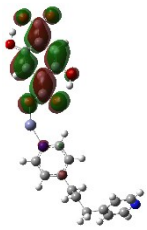
HOMO-5	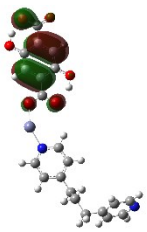	LUMO	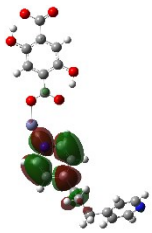

Table S8 Comparison of the performance of various MOF sensors for Al^{3+} and Fe^{3+} ions.

Metals	Materials	Solvents	K_{sv} (M^{-1})	LOD(μM)	References
Al^{3+}	$\{[H_3O]_2[Eu_{2.5}(BTB)_3(OAc)_{0.5}(H_2O)_3]$	DMF	5.57×10^4	100	[1]
	UiO-66-NH_2-SA	Water	-	6.98	[2]
	$[Co_2(dmimpym)(nda)_2]_n$	Water	1.1×10^4	0.7	[3]
	$[Cd(CDC)(L)]_n$	Water	2.6×10^3	61	[4]
	[Cd(PAM)(4-bpdb)1.5]·DMF	Water	2.3×10^4	7.41	[5]
	Zn(DMA)(TBA)	Water	-1.3×10^4	1.97	[6]
	$[Eu_2(ppda)_2(npdc)(H_2O)]\cdot H_2O$	Water	8.68×10^5	109	[7]
	GUPT-2	**Water**	**-1.21×10^4**	**0.269**	**This work**
Fe^{3+}	$[Eu_2(FDC)_3DMA(H_2O)_3]\cdot DMA\cdot 4.5H_2O$	Water	1.1×10^4	2.22	[8]
	$[Zn_2(BDC)_2(4\text{-bpdh})]\cdot 3DMF$	DMF	2.8×10^4	0.2	[9]
	$\{[Cd(L)(SDBA)(H_2O)]\cdot 0.5H_2O\}_n$	Water	3.59×10^4	7.14	[10]
	$\{[Co_3(phen)_2(HL)_2]\cdot(H_2O)_2\}_n$	Water	8.5×10^3	1.79	[11]
	$[Zr_6O_4(OH)_8(H_2O)_4(L^1)_2]$	Water	2.17×10^3	3.79	[12]
	Eu^{3+}@Zn-MOF	Water	1.9×10^4	2	[13]
	$[Cd_2(pbdc)(H_2O)_3]$	Water	1.86×10^5	0.167	[14]
	GUPT-2	**Water**	**1.77×10^4**	**0.446**	**This work**

Notes and references

[1] H. Xu, M. Fang, C.-S. Cao, W.-Z. Qiao, B. Zhao, Inorg. Chem. 55(10) (2016) 4790-4794.

[2] S.-Y. Zhu, B. Yan, Dalton Trans. 47 (2018) 1674-1681

[3] W.-M. Chen, X.-L. Meng, G.-L. Zhuang, Z. Wang, M. Kurmoo, Q.-Q. Zhao, X.-P. Wang, B. Shan, C.-H. Tung, D. Sun, J. Mater. Chem. A, 5(25) (2017) 13079-13085.

[4] S. Chand, M. Mondal, S.-C. Pal, A. Pal, S. Maji, D. Mandal, M.-C. Das, New J. Chem. 42(15) (2018) 12865-12871.

[5] R. Lv, Z. Chen, X. Fu, B. Yang, H. Li, J. Su, W. Gu, X. Liu, J. Solid State Chem. 259 (2018) 67-72.

[6] X. Zhang, X. Luo, N. Zhang, J. Wu, Y. Huang, Inorg. Chem. Front. 4 (2017) 1888-1894

[7] Z. Zhan, X. Liang, X. Zhang, Y. Jia, M. Hu, Dalton trans. 48(5) (2019) 1786-1794.

[8] L. Li, Q. Chen, Z. Niu, X. Zhou, T. Yang, W. Huang, J. Mater. Chem. C 4(9) (2016) 1900-1905.

[9] Y.-D. Farahani, V. Safarifard, J. Solid State Chem. 275 (2019) 131-140.

[10] S. Chen, Z. Shi, L. Qin, H. Jia, H. Zheng, Cryst. Growth Des. 17(1) (2016) 67-72.

[11] Y. Liu, C. Liu, X. Zhang, L. Liu, C. Ge, X. Zhuang, N. Zhang, Q. Yang, Y.-Q. Huang, Z. Zhang, J. Solid State Chem. 272 (2019) 1-8.

[12] B. Wang, Q. Yang, C. Guo, Y. Sun, L.-H. Xie, J.-R. Li, ACS Appl. Mater. Interfaces 9(11) (2017)

10286-10295.

[13] R. Lv, H. Li, J. Su, X. Fu, B. Yang, W. Gu, X. Liu, Inorg. Chem. 56(20) (2017) 12348-12356.

[14] C. Zhang, H. Shi, L. Sun, Y. Yan, B. Wang, Z. Liang, L. Wang, J. Li, Cryst. Growth Des. 18(12) (2018) 7683-7689.